International Journal of Pharmaceutics 628 (2022) 122265

Contents lists available at ScienceDirect

International Journal of Pharmaceutics

journal homepage: www.elsevier.com/locate/ijpharm

Development of a new hydrogel for the prevention of allergic contact dermatitis

Gonçalo Brites [a,b,c], João Basso [a,d], Margarida Miranda [a,d], Bruno Miguel Neves [b,e], Carla Vitorino [a,d,1], Maria T. Cruz [a,b,c,*,1]

[a] Faculty of Pharmacy, University of Coimbra, 3000-548 Coimbra, Portugal
[b] Toxfinder, Lda, 3030-199 Coimbra, Portugal
[c] Center for Neuroscience and Cell Biology - CNC, University of Coimbra, 3004-504 Coimbra, Portugal
[d] Coimbra Chemistry Center, Department of Chemistry, University of Coimbra, 3004-535 Coimbra, Portugal
[e] Department of Medical Sciences and Institute of Biomedicine – iBiMED, University of Aveiro, 3810-193 Aveiro, Portugal

ARTICLE INFO

Keywords:
Hydrogel
Skin barrier
Allergic contact dermatitis
Prevention
Quality by design
Maturation
Permeation
1-Fluoro-2,4-dinitrobenzene
2-Methyl-1,2-thiazol-3(2H)-one

ABSTRACT

Allergic contact dermatitis (ACD) is the most prevalent occupational disease and the most common form of immunotoxicity in humans. Preventing exposure to the triggering allergens is the mainstay of treatment. However, avoidance is not always possible in an occupational setting. From a pathophysiological point of view, a variety of events are involved in the development of ACD, including the formation of immunogenic complexes following the stable association of the allergen with skin proteins, which is thought to be the molecular initiating event responsible for the development of ACD. Previously, the team identified molecules that exhibited higher antiallergic potential due to their capacity to block the interaction between allergens and skin proteins. These assumptions were the starting point for the design of this work aiming to develop and characterize a new hydrogel containing the active ingredients lysine and N-acetyl cysteine under the premises of quality- and safety-by design. Two factorial plannings were established envisioning the optimization of the hydrogel in terms of mechanical and rheological properties. In vitro release and permeation studies supported its skin surface barrier effect. In addition, the selected hydrogel proved to be safe without causing human skin irritation or skin sensitization.

1. Introduction

The skin is a natural barrier that protects the body against a variety of chemical and physical agents, including those caused by ultraviolet (UV) radiation, infectious agents, and chemical components (Parrado et al., 2019). Impairment of skin integrity contributes to the development of several inflammatory skin diseases, including psoriasis, irritant contact dermatitis (ICD) and allergic contact dermatitis (ACD) (Horinouchi et al., 2013; Machado et al., 2020; Yeom et al., 2012). ICD is caused by the proinflammatory and noxious effects of xenobiotics that are normally present in soaps, detergents and solvents and can activate innate skin immunity. In contrast, ACD is a type-IV or delayed-type hypersensitivity reaction caused by low molecular weight (LMW) reactive chemicals (<1000 Da, also called haptens). The majority of haptens displays lipophilic residues, which enable them to cross through the corneal barrier and electrophilic moieties, which account for the establishment of covalent bonds with the nucleophilic residues of endogenous cutaneous proteins. The formation of such hapten–protein complexes is crucial for the activation of the innate immune system, and the efficient priming of T cells that further mediate cutaneous

Abbreviations: ACD, Allergic contact dermatitis; ICD, irritant contact dermatitis; GSH, glutathione; NF-kB, nuclear factor Kb; Lys, Lysine; NAC, N-acetyl cysteine; QTPP, quality target product profile; CQAs, critical quality attributes; CMAs, critical material attributes; FMECA, Failure Mode, Effects and Criticality Analysis; RPN, risk priority number; DoE, design of experiments; AUC, under the force-time curve; LVR, linear viscoelastic region; IVRT, In vitro release testing; IVPT, In vitro permeation studies; DNFB, 1-Fluoro-2,4-dinitrobenzene; MI, 2-Methyl-1,2-thiazol-3(2H)-one; RHE, Reconstructed Human Epidermis; CD54, Cluster of Differentiation 54; CD86, Cluster of Differentiation 86; OECD, Organisation for Economic Co-operation and Development.

* Corresponding author.
E-mail address: trosete@ff.uc.pt (M.T. Cruz).
[1] Equally contributing co-senior authors.

https://doi.org/10.1016/j.ijpharm.2022.122265
Received 11 August 2022; Received in revised form 30 September 2022; Accepted 1 October 2022
Available online 8 October 2022
0378-5173/© 2022 The Authors. Published by Elsevier B.V. This is an open access article under the CC BY-NC-ND license (http://creativecommons.org/licenses/by-nc-nd/4.0/).

inflammation. Haptens may be naturally occurring substances such as urushiol found in the resin of poison ivy, synthetic compounds, dyes, fragrances, drugs, or metal ions, for instance nickel Ni^{2+} and chromium Cr^{3+}. One main concern about this pathology is that once sensitized the individual will always develop ACD after the contact with the allergen, highlighting the relevance of the development of preventive strategies. Indeed, ACD is commonly treated with non-steroidal anti-inflammatory and topical corticosteroids. Nonetheless, the long-term use of topical corticosteroids gives rise to serious adverse side effects, including cutaneous atrophy, telangiectasias, changes in the healing process, intense pruritis, dryness, and burning sensations (Brites et al., 2020; Unzueta and Vargas, 2013).

Once the individual develops the disease, the dermatological treatment can only assist in the healing of the damaged barrier and, in many cases, the environment that led to contact dermatitis cannot be changed so easily. Thus, the disease process continues and requires chronic treatment. One potential strategy is the creation of an artificial barrier, either through barrier creams or gloves, to protect the underlying skin. Unfortunately, gloves themselves can cause ICD or ACD, and might not be appropriate in all household and occupational settings. This calls for the need of new solutions, which may encompass the discovery of new chemical agents and/or formulations (Draelos, 2000).

The incorporation of new or re-discovered active ingredients in barrier and repair formulations, accompanied by active dermatological research, might result in a decreased incidence of household and occupational contact dermatitis (Draelos, 2000). Presently, a plethora of molecules and protocols are under investigation, while some patents and products aiming at the prevention and management of ACD are already available on the market (Brites et al., 2020). Several recent pre-clinical studies reinforce the potential of antioxidants to reduce allergic reactions to some of the most found contact allergens (Coenraads et al., 2016; Jenkinson et al., 2009; Uter et al., 2018). Ascorbic acid, and glutathione (GSH) are among the most studied molecules due to their capacity to block nuclear factor kB (NF-kB) dependent pro-inflammatory signalling mechanisms. Several products are already available on the market containing one or more chelating agents able to block or trap skin allergens (Brites et al., 2020). In this context, screening compounds for their anti-allergic activity assumes critical importance in the development of more effective formulations for the management of ACD. In turn, the properties of the vehicle used for topical delivery of active molecules can assume a noteworthy influence on relevant parameters, including active ingredient delivery, tolerance, and efficacy. Also, the sensorial properties and aesthetic acceptability of these vehicles may impact patient compliance. Ideally, a formulation that fits a routine use should provide an easy and non-greasy application, and allow proper surface evaporation, to prompt a cooling effect and a pleasant sensory appreciation, without compromising skin hydration Fluhr and Darlenski, 2014; Harrison and Spada, 2018.

Hydrogels are hydrophilic polymeric networks capable of absorbing large amounts of water and swelling and shrinking appropriately to allow the controlled release of active compounds (Narayanaswamy and Torchilin, 2019). Indeed, they offer several advantages over other topical formulations, such as creams, lotions, and ointments. Hydrogels hold water by a mechanism similar to a humectant and may be soluble or insoluble in water, depending on their chemical composition (Draelos, 2000). Their high-water content ensures that they are non-greasy, concomitantly providing a better skin feel, improving skin hydration and reducing transepidermal water loss. In addition, evaporation at the surface can lead to a cooling effect on the skin and improves the absorption of active compounds since the contact time tends to be longer than with creams or lotions, allied to an easy removal from the skin or clothing. The appeal of hydrogels in numerous and varied applications is due, in large part, to their mechanical structure highly amenable to modification in several targeted drug delivery hygiene products, wound dressings, contact lenses and tissue engineering (Narayanaswamy and Torchilin, 2019). They are considered very cost-effective and represent an easy-to-use approach to wound healing, overcoming the limitations of multiphasic systems (Harrison and Spada, 2018).

Since the formation of immunogenic complexes following the stable association of the allergen with skin proteins is thought to be the molecular initiating event responsible for the development of skin sensitization, this study aimed to develop a new cost-effective hydrogel able to block the interaction of allergens with skin proteins and functioning like a “chemical glove”. To this end, Lysine (Lys) and N-acetyl cysteine (NAC), herein termed active ingredients, were the compounds that exhibited higher antiallergic potential, as previously reported by the team (Patent application number 20221000002771), and herein selected to be incorporated in the hydrogel-based device. Accordingly, these active ingredients can chemically sequester skin allergens thus avoiding their interaction with skin proteins and, consequently, inhibiting the formation of the immunogenic complexes responsible for the early cellular and molecular mechanisms triggering the development of ACD. Underlying a sustainable development assumption, a preliminary risk assessment was first performed to identify the most impacting variables of hydrogel quality. The composition of the hydrogel was then set forth based on a two-step factorial planning, considering mechanical and rheological properties, respectively. Since the active molecules must be released and remain active in the hydrogel and have to exert their effect on the surface of the skin, the formulation was subsequently characterized in terms of their release and permeation behavior. Finally, the safety and efficacy of the device were assessed based on *in vitro* cellular outcomes.

2. Materials and methods

2.1. Materials

Sodium hydroxide (NaOH) and disodium hydrogen phosphate (Na_2HPO_4) were obtained from Merk (Darmstadt, Germany). Disodium edetate (Na_2EDTA) was purchased from Sigma (Missouri, EUA). Benzoic acid and potassium dihydrogen phosphate (KH_2PO_4) were purchased from PanReac AppliChem ITW Reagents (Chicago, USA), while isopropanol was acquired from Lab Chem (Zelienople, USA). Carbopol® Ultrez NF 10 was kindly donated by Lubrizol (Ohio, USA). N-acetyl-l-cysteine sigma grade, A7250 (NAC) and L-Lysine, L5501 (Lys) were purchased from Sigma-Aldrich (Missouri, EUA). Fenistil gel (used as reference) was acquired from a local pharmacy. Water ($\Omega = 18.2$ MΩ. cm, TOC < 1.5 μg/L) was ultrapurified (Sartorius®, Göttingen, Germany) and filtered through a 0.22 μm nylon filter before use. All other chemicals were of analytical grade or equivalent.

2.2. Methods

2.2.1. Hydrogel development - quality by design approach

Sustainably designing a formulation demands a critical and systematic analysis of the potential factors impacting product quality, covering several sequential and integrated steps, described in the sections that follow.

2.2.1.1. Definition of QTPP. The quality target product profile (QTPP) was established, prospectively comprising certain hydrogel quality features that ideally should be reached, considering product efficacy, safety and quality. Potential critical quality attributes (CQAs) were identified as a set of the QTPP that should be within an appropriate specification to ensure hydrogel quality achievement.

2.2.1.2. Risk assessment. To identify critical material attributes (CMAs), a Failure Mode, Effects and Criticality Analysis (FMECA) was constructed to quantify the risk or failure mode(s) linked to the intended formulation and to evaluate their impact on hydrogel CQAs. Accordingly, risk quantification relies on the severity (S), probability of

occurrence (O) and detectability (D) of each parameter, in a numerical scale from 1 to 5, with 1 being the lowest severity, probability and undetectability and 5 the highest. For each factor, the rank and prioritization of the risk were conducted according to the risk priority number (RPN) given by RPN = S × O × D (Basso et al., 2021). The factors presenting higher RPN values were subjected to a further optimization process.

2.2.1.3. Design of experiments. The design and optimization of the hydrogel formulation were set forth considering two full factorial plannings, 2^k, with k = 3 factors, including a low and a high level, coded as –1 and + 1 level, respectively. Note that CMAs were selected according to risk assessment. The first design of experiments (DoE 1) was directed to the establishment of the hydrogel base composition, taking into consideration the suitable properties for a routine skin application. Three critical formulation or material attributes (CMAs) were considered, namely, carbomer concentration (Carbopol® Ultrez NF 10, X1), alkalizing agent amount (NaOH, X2) required to ensure a certain pH, and antioxidant concentration (Na_2EDTA, X3). As responses or independent variables, mechanical properties, including responses extracted from spreadability and texture profile analyses were examined (Table 1). The second design of experiments (DoE 2) aimed at optimizing the hydrogel microstructure after the incorporation of the active compounds. In this case, the concentration of isopropanol (X1′) and carbomer (X2′), as well as the presence of NAC and LYS (X3′) were considered as CMAs. As response, the rheological behavior was thoroughly inspected. The selection of range factors relied on the technological usage level. A total of eight formulations in each DoE was prepared.

Both Student *t*-test and ANOVA were performed to examine the statistical significance of the terms in the regression model and to inspect the validity of the model fittings, respectively. For the Student *t*-test, a 95% level of confidence ($\alpha = 0.05$) was assumed, whereas, in ANOVA, a value of $p < 0.05$ was considered statistically significant. The optimal conditions were selected based on the quadratic polynomial function 1.

$$Y = \beta_0 + \beta_1 X_1 + \beta_2 X_2 + \beta_3 X_3 + \beta_{12} X_1 X_2 + \beta_{13} X_1 X_3 + \beta_{23} X_2 X_3 \quad (1)$$

where Y is the measured response associated with each factor level combination, β_0 is the response in the absence of effects, β_1, β_2 and β_3 are the linear coefficients of the respective factors and β_{12}, β_{13} and β_{23} are the interaction coefficients between the respective factors. The fitted models were retrieved using JMP Pro 16 Software (SAS Institute, USA).

Table 1
Independent and dependent (responses) variables of experimental designs and respective codification.

	CMA		Level −1	Level + 1
DoE 1	Carbopol® Ultrez NF 10	**X1**	0.5 (% w/w)	1 (% w/w)
	NaOH	**X2**	3.5 (pH)	5.5 (pH)
	Na_2EDTA	**X3**	0.01 (% w/w)	0.1 (% w/w)
	Responses	Texture profile analysis (compressibility, hardness, adhesiveness, cohesiveness, elasticity)Spreadability (firmness, work of shear)		
DoE 2	Isopropanol	**X1′**	0 (% w/w)	30 (% w/w)
	Carbopol® Ultrez NF 10	**X2′**	1 (% w/w)	1.25 (% w/w)
	NAC / LYS	**X3′**	0 (% w/w)	0.02 (% w/w, each)
	Responses	Rheological behaviour (viscosities at specified shear stresses, comprising zero-shear, shear thinning and infinite-shear viscosity regions; rotational yield point; thixotropic relative area; linear viscoelastic region; oscillatory yield point; storage modulus, loss modulus, and loss tangent at different frequencies).		

2.2.2. Hydrogel preparation

Hydrogel formulations were prepared following a conventional manufacturing method. Briefly, and considering DoE 1 conditions, the carbomer was added to an aqueous solution containing Na_2EDTA and benzoic acid (0.1% w/w) under mechanical agitation (HS-30D mechanical stirrer, Witeg, Germany), at 500 rpm, for 1 h, to enable complete polymer hydration. Formulations were subsequently neutralized, using a NaOH 4 M solution. As for DoE 2, NAC and LYS were dissolved in the initial aqueous solution, containing Na_2EDTA and benzoic acid (0.1% w/w), to which the carbomer was added under mechanical agitation (HS-30D mechanical stirrer, Witeg, Germany), at 800 rpm, for 1 h. Isopropanol (or the equivalent volume of water) was then incorporated into the formulations, with pH being adjusted with NaOH 4 M solution (digital pH C3010 Multiparameter Analyzer, Consort bvba, Belgium). Hydrogels were stored at 25 °C.

2.2.3. Hydrogel characterization

2.2.3.1. Texture profile analysis. Texture profile analysis was carried out in a Texture Analyzer TA.XT Plus (Stable Micro Systems Ltd., UK), equipped with an analytical probe (P/10, 10 mm Delrin), which was depressed twice into the sample at a 5 mm/s rate up to a 15 mm depth, with 15 s of delay between the two consecutive compressions. Hydrogel samples were placed in cylindrical tubes of the same dimension, at a fixed height. Nine replicates were performed at 32 °C, to simulate skin surface temperature for all formulations. Data collection and calculation were performed using the Texture Exponent 6.1.16.0 software package of the instrument. From the force–time curves, the following mechanical parameters can be determined: (i) hardness, given by the maximum peak force during the first compression cycle; (ii) compressibility (i.e., the work required to deform the sample during the first compression of the probe), calculated from the area under the force–time curve 1 (AUC1); (iii) adhesiveness (the work required to overcome the attractive forces between the surface of the sample and the surface of the probe), indicated as the negative force area for the first compression cycle and calculated from the area under the force–time curve 2 (AUC2); (iv) cohesiveness (the ratio of AUC2 and AUC1, in which both compressions are separated by a recovery period); and (v) elasticity, which corresponds to the ratio of the time required to achieve maximum structural deformation on the second compression cycle, to that on the first compression cycle (Hurler et al., 2012; Vitorino et al., 2014).

2.2.3.2. Spreadability. To evaluate the spreadability of the hydrogels, the TTC Spreadability Rig was previously calibrated for weight and distance. Accordingly, the probe was placed precisely 25.0 mm above the flask cone, where the hydrogels are placed for analysis. The evaluation consists of the penetration of the gel with the cone probe, at a velocity of 3.0 mm/s, to a depth of 2 mm above the sample holder surface. During penetration, the force increases until the point of maximum penetration depth, which can be inferred as the firmness value. The curve integral, corresponding to the work of shear, indicates the extent of the area to which gels readily spreads when applied to the skin. This is a relevant parameter since the formulation effect is also dependent on its spreading value (Kryscio et al., 2008).

2.2.3.3. Rheological characterization. The rheological behaviour of the hydrogels was analysed using a Haake™ MARS™ 60 Rheometer (ThermoFisher Scientific, Germany) with a controlled temperature maintained by a thermostatic circulator and a Peltier temperature module (TM-PE-P). Data were analysed with Haake Rheowin® Data Manager V.4.82.0002 (ThermoFisher Scientific, Germany). The temperature was maintained at 32 °C throughout the experimental analyses, with a sample hood being used to minimise temperature fluctuations. For each test, approximately 1.0 g of each hydrogel was placed on the lower plate through a positive displacement syringe, before slowly

lowering the upper geometry to the predetermined trimming gap of 1.1 mm. After trimming, the geometry gap was set at 1 mm. Rotational and oscillatory measurements were performed sequentially on each sample for a thorough rheological characterization. All rheological studies were performed 6 times.

Rotational Measurements.

Rotational measurements were conducted using cone (P35 2°/Ti; 35 mm diameter, 2° angle) and plate (TMP 35) geometry configuration. Viscosity curves [$\eta = f(\tau)$] were recorded by a control rate flow step from 0.1 to 50 s^{-1} for 10 min. Apparent viscosity was obtained at a shear stress of 25, 50, 100 and 200 Pa. Additional flow curves were generated by ramping the shear rate from 0.01 to 300 s^{-1} over 3 min (ascendant curve) and then from 300 to 0.01 s^{-1} during 3 min (descendent curve). The thixotropic behaviour was estimated by considering hysteresis loop areas (S_R, Pa/s).

Oscillatory Measurements.

The viscoelastic properties were investigated using a P35/Ti plate geometry. An amplitude sweep test between 0.01 and 600 Pa at 1 Hz was firstly conducted to estimate the linear viscoelastic region (LVR) plateau, yield point ($\tau_{0,OSC}$) and flow point (τ_f). Afterwards, a frequency sweep analysis was conducted, within the LVR plateau. The storage modulus (G'), loss modulus (G'') and loss tangent (tan) were calculated at 1, 10 and 100 Hz.

2.2.3.4. Assay of NAC and LYS. N-acetyl-l-cysteine and L-Lysine, included in the hydrogel were extracted with mobile phase under agitation for 5 min. Samples were filtered (0.45 μm) and quantified by reversed-phase high-pressure liquid chromatography (RP-HPLC) following the procedure described in Section 2.2.3.7.

2.2.3.5. In vitro release testing (IVRT). Release studies of the hydrogels were performed on static vertical Franz cells (PermeGear, Inc., USA), with a diffusion circular area of 0.636 cm^2 and a receptor compartment of 5 mL. For that, infinite dose conditions (1 g) of the formulations were applied in the upper compartment, separated from the receptor by a cellulose membrane (MWCO ≈ 14 000 Da, flat width 33 mm, Sigma-Aldrich), previously hydrated in ultrapurified water for at least 30 min. Before the experiments, the system was equilibrated for a minimum of 30 min. The release medium was composed by phosphate buffer pH 5.5 (guaranteeing the maintenance of sink conditions) and continuously stirred at 600 rpm, at 37 °C. A circulating water bath maintained the membrane surface temperature at 32 ± 1 °C. During the release studies, the donor compartment, as well as the receptor sampling arm, were carefully covered to avoid medium evaporation, as well as to conduct the experiments under occlusive conditions. At predetermined time points (0.25, 0.5, 0.75, 1, 2, 3, 4 and 6 h), 300 μL of the medium were withdrawn and immediately replenished with fresh medium. NAC and LYS were quantified by HPLC, as described in section 2.2.3.7. Release studies were conducted considering n = 6 samples.

The cumulative amount (*Qn*) of NAC and LYS released over time was calculated according to equation (2):

$$Qn(\mu g/cm^2) = \frac{Cn.V_0 + \sum_{i=1}^{n=l} Ci.Vi}{A} \quad (2)$$

where *Cn* is the NAC or LYS concentration of the receptor medium at each sampling time, *Ci* is the NAC or LYS concentration of the i^{th} sample, *A* the effective diffusion area (0.636 cm^2), and *Vo* (5 mL) and *Vi* (300 μL) the volumes of the receptor compartment and the collected sample, respectively. The release rates were retrieved from the slope of the linear regression obtained by plotting the cumulative amount of NAC or LYS diffused per cm^2 as a function of the square root of time. Additionally, mass balance studies were performed to characterize the extent of dose depletion, according to equation (3):

$$DD(\%) = \frac{Qf}{Qi}.100 \quad (3)$$

where *Qf* reflects the average cumulative amount released at the end of the assay and *Qi* the initial amount of NAC or LYS placed on the membrane.

2.2.3.6. In vitro permeation studies (IVPT). The same vertical diffusional system of IVRT studies was used to evaluate the potential *in vitro* penetration of the active molecules. Human surgical skin pieces (female, type 3 skin, 57 years old, arm tissue) were surgically removed at Central Lisbon University Hospital Centre, after the approval of the Bioethics Committee, and processed as described in (Miranda et al., 2020). Written informed consent was obtained from the participant (Process number 447/2017). One day before the experiments, frozen epidermal specimens were left to thaw at room temperature. Afterwards, the skin sheets, with the *stratum corneum* side facing up, were gently placed on glass flasks filled with ultrapurified water and left to stabilize overnight, at 4 °C. On the day of the experiments, the epidermis was carefully transferred to each Franz cell, with barrier integrity being tested by measuring the transepidermal water loss (TEWL), recurring to a vapometer (Delfin Technology, Kuopio, Finland). Indications of stretch - marks, physical damage, or a TEWL value higher than 20.0 g/m^2/h led to the rejection of the epidermic piece (Shin et al., 2020). Similarly, to IVRT, infinite dose conditions (1 g) of the formulations were applied to the donor compartment. The receptor medium, composed of 5 mL of phosphate buffer pH 5.5, was continuously stirred at 600 rpm with all experiments being conducted in a temperature-controlled water bath to ensure a skin surface of 32 ± 1 °C. Nonetheless, the assay was conducted under non-occlusive conditions, to mimic clinical use (Kamal et al., 2020). At predetermined time points (0.25, 0.5, 0.75, 1, 2, 3, 4, 6, 8 and 24 h), 300 μL of the medium were withdrawn and immediately replenished with fresh medium. NAC and LYS were quantified by RP-HPLC, as described in section 2.2.3.7. Permeation studies were conducted considering five replicates.

2.2.3.7. NAC and LYS quantification. NAC and LYS were quantified by reversed-phase high-pressure liquid chromatography (RP-HPLC), using a Shimadzu LC-2010HT chromatographic system, equipped with a LC-20AD quaternary pump, a SIL-20AHT autosampler, a CTO-10AS over and an SPD-M2OA photodiode array detector. The separation of the analytes was achieved on a Surf C_8 column, with 3 μm of particle size, 4.6 mm of internal diameter and 150 mm of length (ImChem Sarl, Portugal) under the following conditions: isocratic mode, at 30 °C, with a mobile phase consisting of 95:5 (v/v) phosphate buffer 25 mM pH 3.0: acetonitrile, at 0.8 mL/min. Using an injection volume of 50 μL, NAC and LYS were determined at 200 and 215 nm and eluted at 5.4 and 2.2 min, respectively. During the analyses, an external calibration curve with six different NAC and LYS standards was drawn through the plotting of peak area as a function of the concentration, following a $1/x^2$ weighting factor. A determination coefficient, R2 > 0.999 was considered for attaining linearity.

2.2.4. Biological activity studies

2.2.4.1. Cell culture. For viability studies, the human epidermal keratinocyte cell line HaCaT (CLS Cat # 300493), representative of the epidermis, was cultured in DMEM medium supplemented with 10% (v/v) of heat-inactivated FBS (both from Life Technologies, California, USA), 25 mM glucose, 35.9 mM sodium bicarbonate, 100 U/mL penicillin and 100 μg/mL streptomycin (all from Sigma-Aldrich, Missouri, USA). Cells were kept at 37 °C in a 5% CO_2 humidified atmosphere. Subculturing was performed according to the manufacturer's recommendations and morphological cell alterations were monitored by microscope observation. For maturation studies, the human monocytic cell line THP-1 (ATCC® TIB-202 ™, American Type Culture Collection, Manassas, VA, USA) was used. The cells were cultured and maintained at a cell density between 0.3 × 10^6 and 0.5 × 10^6 cells/mL in RPMI 1640

supplemented with 10% (v/v) of heat-inactivated FBS, 25 mM glucose, 10 mM HEPES (4-(2-hydroxyethyl)-1-piperazineethanesulfonic acid), 1 mM sodium pyruvate, 100 U/mL penicillin, 100 μg/mL streptomycin and 0.05 mM 2-mercaptoethanol. The maintenance of the cells was done according to the manufacturer's instructions.

2.2.4.2. Cellular metabolic activity/viability studies. The metabolic activity of HaCaT cells was evaluated using the resazurin reduction assay, as previously described (O'Brien et al., 2000). Briefly, cells were plated at a density of 0.5×10^6 cells/mL, specifically 0.1×10^6 cells/well in a 96-well plate (200 μL/well) and subsequently exposed to the hydrogel alone (208 mg) or the hydrogel containing several concentrations of the active ingredients (20, 10, 5, 2.5, 1.25, 0.6, 0.3 and 0.1 mM), for 24 h. Resazurin (Sigma-Aldrich, USA) solution (50 μM), prepared with sterile phosphate buffer solution, was added to each well in the last 4 h of the incubation. Then, the absorbance was read at 570 and 620 nm with a Microplate Absorbance Spectrophotometer BioTek® Synergy HT (Winooski, EUA).

2.2.4.3. Effectiveness of the selected formulation: Maturation in THP-1 cell line. Previously to the experiments, cell concentration was adjusted to 0.5×10^6 cells/mL and left to stabilize overnight at 37 °C. Then, 1.5 mL of cell culture were plated in each well of a 12-well plate and the active ingredients NAC and LYS were added at a final concentration of 10 mM. After a pre-incubation period of cells with the active ingredients (1 h at 37 °C), two strong allergens, 1-Fluoro-2,4-dinitrobenzene (DNFB, CAS 70-34-8) and 2-Methyl-1,2-thiazol-3(2H)-one (MI, CAS 2682–20-4) were added (final concentration of 8 and 100 μM, respectively) and used as positive controls. Cells were further incubated for 24 h at 37 °C. Then, cells were washed twice with 1 mL of PBS containing FBS 1% (v/v) and centrifuged twice at 300*g* for 5 min. Cells were further resuspended in 700 μL of the previous solution and 200 μL were collected for two microtubes: 100 μL for the unstained condition and 100 μL for the stained condition. The stained condition contains 3 μL of each antibody: anti-CD86 (clone IT2.2, reference 305414) and anti-CD54 (clone HA58, reference 353111), purchased from Biolegend (San Diego, CA, EUA). After 30 min of incubation at 4 °C, cells were washed, resuspended in 100 μL of PBS containing FBS 1% (v/v), and further analysed by flow cytometry, using the BD Accuri™ C6 cytometer (San Jose, CA, EUA).

2.2.4.4. Irritation on human skin. Skin irritation was evaluated using the SkinEthic™ Reconstructed Human Epidermis (RHE) model (EPISKIN Laboratories, Lyon, France), in compliance with the OECD Test Guideline No. 439 - *In Vitro* Skin Irritation: Reconstructed Human Epidermis Test Method. The RHE model consists of a differentiated three-dimensional epidermal tissue of human keratinocytes grown on a 0.5 cm^2 surface inert polycarbonate filter in a chemically defined medium at the air–liquid interface. Two specific media provided by EPISKIN were used: maintenance and growth media. On the day of receipt, the SkinEthic™ RHE inserts were transferred into 6-wells plates filled with 1 mL of maintenance medium and stored in an incubator at 37 °C, under a 5% CO_2-95% air atmosphere, for 24 h. For the experiments, SkinEthic™ RHE inserts were placed with maintenance medium in 24-well plates (300 μL/well), or with 10 and 100 mM of hydrogel enriched with NAC and LYS, or hydrogel vehicle (hydrogel without the active ingredients). All the tested conditions were topically applied on the surface of an insert on three tissues replicates, for 42 min at RT. The experiment also included other inserts treated with PBS or SDS 5% (w/v in water), used as negative and positive controls, respectively. After the exposure time, the SkinEthic™ RHE inserts were rinsed 25 times with 1 mL PBS and transferred to 6-well plates with a growth medium (2 mL/well) to be incubated for 42 h at 37 °C, under a 5% CO_2 with 95% air atmosphere. Tissue viability was assessed using the MTT (3-(4,5-dimethylthiazol-2-yl)-2,5-diphenyltetrazolium bromide) assay. For that, tissues were incubated with MTT (1 mg/mL) at 37 °C for 3 h; then, the MTT solution was removed, and formazan crystals were dissolved with isopropanol. The absorbance was measured at 570 nm using a SpectraMax Plus 384 Spectrophotometer. The results achieved on three tissue replicates were expressed as a percentage (%) of the absorbance value obtained in the negative control, which was considered 100%, and were graphically presented as % of tissue viability. If the tissue viability value is $< 50\%$, the samples are classified as irritants.

3. Results and discussion

Under the Quality by Design umbrella, the definition of the quality target product profile (QTPP) is the first step to obtaining the optimal device, in this case, a hydrogel with the desired characteristics and performance for topical application. Bearing in mind the intended activity, that is, to avoid the contact of allergens with the skin while inhibiting the maturation and prevention of allergic contact dermatitis, the QTTP was established (Table 2). Note that the hydrogel should exert its activity via two independent mechanisms: (i) by creating a physical barrier at the skin surface, it should decrease the potential contact with allergens; (ii) the active molecules incorporated in the hydrogel should be able to decrease allergen activity. This preliminary evaluation allowed the identification of potential critical quality attributes (CQAs) (Simões et al., 2019).

The risk assessment on the critical material attributes (CMAs) was further performed through a failure mode, effects, and criticality analysis (FMECA). This evaluation, based on prior knowledge, enables to quantify and rank formulation variables according to their preliminary impact on potential hydrogel CQAs (Table 3). The influence of critical process parameters was not herein inspected, given the low complexity of the manufacturing process and the overall water solubility of the components.

According to the risk priority number determined for each variable, risk acceptance for potential CMAs was ranked as intolerable, unacceptable and acceptable. Consequently, two sequential factorial designs were then outlined: DoE 1 envisioning the design of definition of the hydrogel base and DoE 2 devoted to optimizing the microstructure after incorporating NAC and LYS, as active molecules.

3.1. Designing a hydrogel-based formulation

The optimal conditions for establishing the hydrogel base composition were selected using a two-level, three-variable full factorial design, denoted as DoE 1. The most representative CMAs were identified, according to risk assessment and include the carbomer, alkalinizing agent and antioxidant concentrations (Table 1).

The carbomer Carbopol® Ultrez 10 NF, a hydrophilic, high molecular weight, crosslinked polyacrylic acid polymer, was chosen as a thickener agent, due to its self-wetting properties and low dusting, which makes it extremely easy to use for efficient processing. It is also an efficient rheology modifier, able of providing high viscosity and forms clear gels or hydro-alcoholic gels (Kulkarni and Shaw, 2016). Nonetheless, carbomers in liquid formulations may react with oxygen, thus leading to a permanent reduction or loss of viscosity. Certain metals present in water (particularly, trace levels of iron and other transition metals) catalyze this reaction, inducing carbomer degradation with consequent loss of the hydrogel integrity (Lubrizol, 2011). These phenomena may be overcome by adjusting the formulation pH and/or by using additives to help prevent degradation. Na_2EDTA is often used as a chelating agent to prevent this undesirable effect, while NaOH is used as a neutralizer, thus prompting the desirable consistency. These aspects determined their selection as CMAs with potential impact on the mechanical properties of the hydrogel. The definition of each CMA concentration range was established based on common levels of usage.

Textural characteristics of the hydrogels, specifically, hardness, compressibility, adhesiveness, cohesiveness, elasticity and spreadability were evaluated by texture profile analysis. These mechanical properties

Table 2
Quality target product profile (QTPP) of the hydrogel.

Quality Attributes	Target	CQA?	Justification
Dosage form	Gel	No	The hydrogel high water content ensures that the dosage form is not greasy, it promotes a better skin sensation, improves skin hydration and reduces transepidermal water loss. Surface evaporation can lead to a cooling effect on the skin. It is also easy to remove from the skin or clothing.
Route of administration	Topical	No	Related to the disease pathophysiology.
Dosage	0.2% w/w	No	Relies on the purpose of the drug product. Based on optimization studies.
Dosage form design	Hydrogel with NAC and LYS dissolved	No	Both active molecules show an increased water solubility. Hydrogels are topical forms with increased water content, able to incorporate NAC and LYS.
Assay	90–110% of the labelled claim	No	Influence on activity efficacy.
Physicochemical attributes			
Appearance	Homogeneous	No	Hydrogels are monophasic pharmaceutical forms. Not directly interlinked with safety and efficacy
Color	Colorless	No	Hydrogel excipients and active molecules lack color. Not directly interlinked with safety and efficacy
Odor	No objectionable odor	Yes*	Impact on patient compliance.
pH	Compatible with skin	No	Prevent local irritation.
Texture analysis	Appropriate for skin application	Yes	Impact on gel spreadability and acceptability.
Rheological Behavior	Appropriate for skin application	Yes	Impact on *in situ* gel persistence and consequently, on the protection afforded. Effect on active agent release behavior at the microstructure level.
Product Performance			
In vitro release testing	Controlled release	Yes	A sustained release of the active molecules ensures efficacy throughout time.
In vitro permeation testing	Preferable accumulation at the skin surface	Yes	Active molecules should be retained on skin surface, and not permeate through the epidermis.
Physicochemical stability	Appropriate stability	Yes	To ensure patient application.

* Despite having been considered a potential CQA, its assessment is out of the scope of this work.

of the formulations are presented in Table 4.

An overall model analysis indicates a better fitting achieved for spreadability than texture profile parameters. This is aligned with **Figure S1**, **Supplementary Material**, which exhibits the observed *vs*. predicted values for CQAs showing better goodness of fit. Moreover, Fig. 1 indicates that isolated coefficient terms are, in the vast majority, statistically significant. The assessment of ANOVA, performed for model fitness (**Table S1**, **Supplementary Material**), also reveals the appropriateness of the designated mathematical model for predicting the responses.

By inspecting the influence of CMAs, it is observed that the NaOH concentration (X2) required for attaining a particular formulation pH exerts the major effect on mechanical properties, followed by the carbomer (X1) and, ultimately, the Na_2EDTA (X3), as indicated in Fig. 1. Different effects were, however, denoted. While a higher concentration of NaOH and carbomer render a higher gel firmness (F6 and F8), the opposite behaviour was observed for Na_2EDTA, as the coefficients present negative values. This indicates that increasing Na_2EDTA leads to a decreased response in gel firmness and work of shear (Fig. 1), which is attributed to the hydration of polymer chains that are interconnected by crosslinks. Their swelling induces a partial uncoilment, that along with the ionization process leads to electrostatic repulsion, thus forming irreversible agglomerates (Varges et al., 2019). Such trend is reinforced by the β_{12} interaction term, which evidences the synergistic effect prompted by these CMAs on the gel mechanical properties. This is also imparted by the pH effect, with lower pH influencing the formation of a gel that is comparatively less swollen and occupies a slightly smaller volume, indicating a less compacted gel network structure alternatively to a more fluid structure (Kolman et al., 2021).

The desirability approach was employed for CMA optimization aiming at a maximization of all CQAs. After conducting the experiments and fit response models for all responses, the desirability approach involves the following steps: (i) defining individual desirability functions for each response ($di(Y_i)$) and (ii) maximizing the overall desirability with respect to the controllable factors. The desirability (D) function is described as the weighted geometric mean for several responses, or alternatively, a value comprised between 0 and 1, per response. A value of D different from zero indicates that all responses are in a desirable range, whilst a value close to 1 is pointed out as the combination of the different criteria considered optimal. As such, when $D = 1$, it means that the response values are close to the target ones (Kalariya et al., 2017) (Miranda et al., 2019)(Kamboj and Rana, 2016). According to Fig. 2, the maximum desirability (0.683) was found for the formulation containing the highest carbomer (level 1, 1% w/w) and alkalizing agent concentration (level 1, pH 5.5), and the lowest chelating agent (level −1, 0.01% w/w) concentration.

A parallel approach for establishing the composition of the hydrogel-based formulation was conducted by considering Fenistil gel 1 mg/g as reference, due to the inexistence of specification values for these attributes. The white regions displayed in contour profilers (Fig. 3**)** correspond to the optimal experimental conditions, extracted from the overlay of the responses, wherein every single point represents a combination of two variables, whose result is a gel formulation compliant with the predefined acceptable limits. Note that these regions consistently comprise the coordinates (1;1;-1), previously identified with the desirability function and correspond to formulation F6. Therefore, this consubstantiated the definition of the hydrogel base composition.

3.2. *Optimizing hydrogel formulation*

The incorporation of NAC and LYS in the hydrogel composition may induce alterations in its microstructure. The DoE 2 aimed at scrutinizing this effect, along with fine-tuning the hydrogel rheological properties towards an improved skin application.

Isopropyl alcohol was herein introduced to provide somehow surface evaporation and *in situ* active accumulation and for active odor masking properties. Apart from the retention, a pleasant cooling, non-greasy effect on the skin was also sought. To balance the viscosity, an adjustment in the carbomer concentration was conducted. Note that viscosimetric measurements provide noteworthy information regarding formulation, application/sensorial properties, structural stability during shelf life, as well as useful information on the release of the active agent from the vehicle. Again, this planning considered eight different hydrogel formulations, which were thoroughly characterized through rotational and oscillatory rheological measurements (Fig. 4). Rotational tests support the evaluation of small periodic deformations that determine breakdown or structural rearrangement and hysteresis, while oscillatory tests allow the analysis of material viscoelastic properties when they are exposed to small-amplitude deformation forces (Simões et al., 2020).

Table 3
Failure Mode, Effects and Criticality Analysis (FMECA) tool presenting initial risk assessment for hydrogel formulation.

Variables	Failure Mode	Failure Cause	Failure Effect	S	O	D	RPN	Acceptance
NAC and LYS (active molecules)	Low concentration; Oxidation susceptibility	Potential degradation	Lack of activity	5	2	3	30	Intolerable
Carbopol® Ultrez NF 10 (thickener)	Inappropriate hydration	Reduced stirring time	Inappropriate microstructure	5	2	2	20	Unacceptable
NaOH (alkalizing agent)	Concentration inaccuracy	Weighing error	Impact on active release and permeation	4	1	4	16	
Na_2EDTA (antioxidant)			Chemical instability	4	2	2	16	
Benzoic acid (antimicrobial preservative)				5	2	1	10	
Isopropanol (solvent)			Microbiological instability; impact on rheological behavior	5	2	1	10	Acceptable
Ultrapurified water (solvent)				5	2	1	10	

Key: S, Severity; O, Occurrence; D, Detectability; RPN, Risk Priority Number.

Table 4
Mechanical properties of the formulations extracted from the texture profile analysis (TPA) and spreadability tests, ($6 \leq n \leq 9$).

				TPA						Spreadability
Formulation	X1	X2	X3	Compressibility (g.s)	Hardness (g)	Adhesiveness (g.s)	Cohesiveness (g.s)	Elasticity (Pa)	Firmness (g)	Work of shear (g.s)
F1	−1	−1	−1	0.30 ± 0.27	2.4 ± 0.1	−3.9 ± 1.5	−0.5 ± 0.9	0.11 ± 0.09	6.9 ± 0.3	4.0 ± 1.4
F2	−1	+1	+1	5.9 ± 0.3	5.1 ± 0.4	−12 ± 3	0.90 ± 0.05	0.94 ± 0.07	86 ± 23	64 ± 17
F3	−1	−1	+1	1.6 ± 0.5	3.3 ± 0.6	0.6 ± 1.3	0.6 ± 0.7	0.5 ± 0.4	12.0 ± 0.9	8.1 ± 1.9
F4	−1	1	−1	7.6 ± 1.9	11.5 ± 1.1	−7.1 ± 1.1	6.1 ± 1.8	0.64 ± 0.11	8.5 ± 0.3	7.3 ± 1.4
F5	+1	−1	−1	3.3 ± 0.4	3.4 ± 0.3	0.0 ± 2.4	0.9 ± 0.1	0.9 ± 0.1	31 ± 5	12 ± 5
F6	+1	+1	−1	14 ± 5	17 ± 5	−13 ± 5	0.98 ± 0.09	0.66 ± 0.10	372 ± 36	343 ± 23
F7	+1	−1	+1	1.44 ± 0.20	2.7 ± 0.3	0.0 ± 2.6	1.0 ± 0.4	0.74 ± 0.15	6.7 ± 1.0	5.4 ± 2.3
F8	+1	+1	+1	12 ± 3	17.1 ± 1.9	−14 ± 9	0.7 ± 0.6	0.6 ± 0.3	300 ± 76	277 ± 70
Reference	–	–	–	9.3 ± 2.3	9.7 ± 1.1	−17 ± 10	0.967 ± 0.028	0.77 ± 0.10	111 ± 10	90 ± 10

Key: X1, Carbomer; X2, NaOH; X3, Na_2EDTA. Note that for adhesiveness, values should be regarded in modulus.

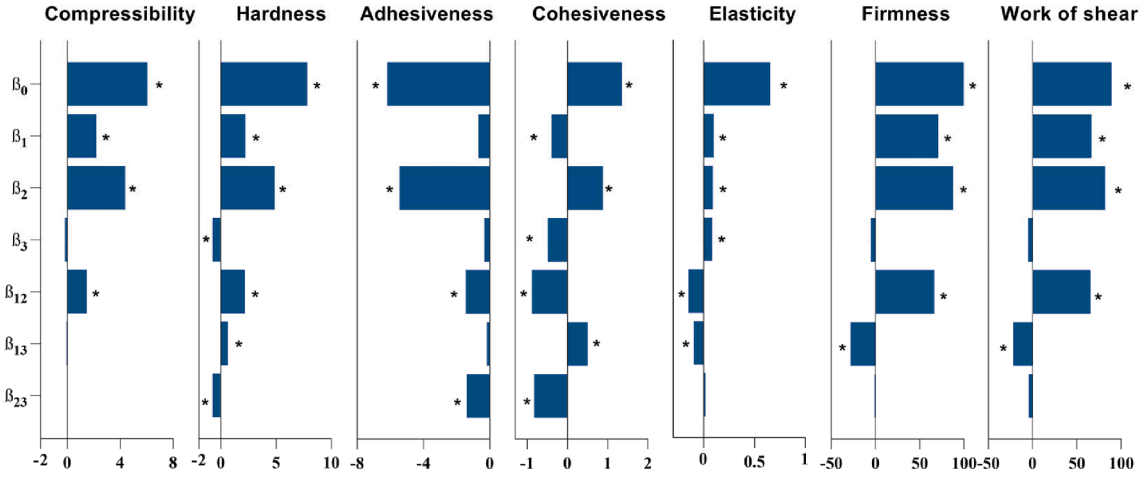

Fig. 1. Coefficients for mechanical parameters evaluated in DoE 1 (compressibility; hardness; adhesiveness; cohesiveness; elasticity; firmness and work of shear). Key: β0, intercept; β_1, Carbomer; β_2, NaOH; β_3, Na_2EDTA; β_{12}, Carbomer*NaOH; β_{13}, Carbomer*Na2EDTA; β_{23}, NaOH*Na2EDTA. *Statistical significant coefficients, as extracted from Student's *t*-test analysis.

While the former was considered to investigate the effect of each formulation component on the viscosity at distinct stresses, the latter aimed to study the structure of the materials under slight deformations.

As shown in Fig. 4**A and** Table 5, formulations evidenced a pseudoplastic behavior, consistent with a non-Newtonian and shear thinning pattern, that is, a decrease in apparent viscosity was observed as shear stress is increased. The Newtonian range, corresponding to the first plateau in the rheograms was, however, distinct depending on the

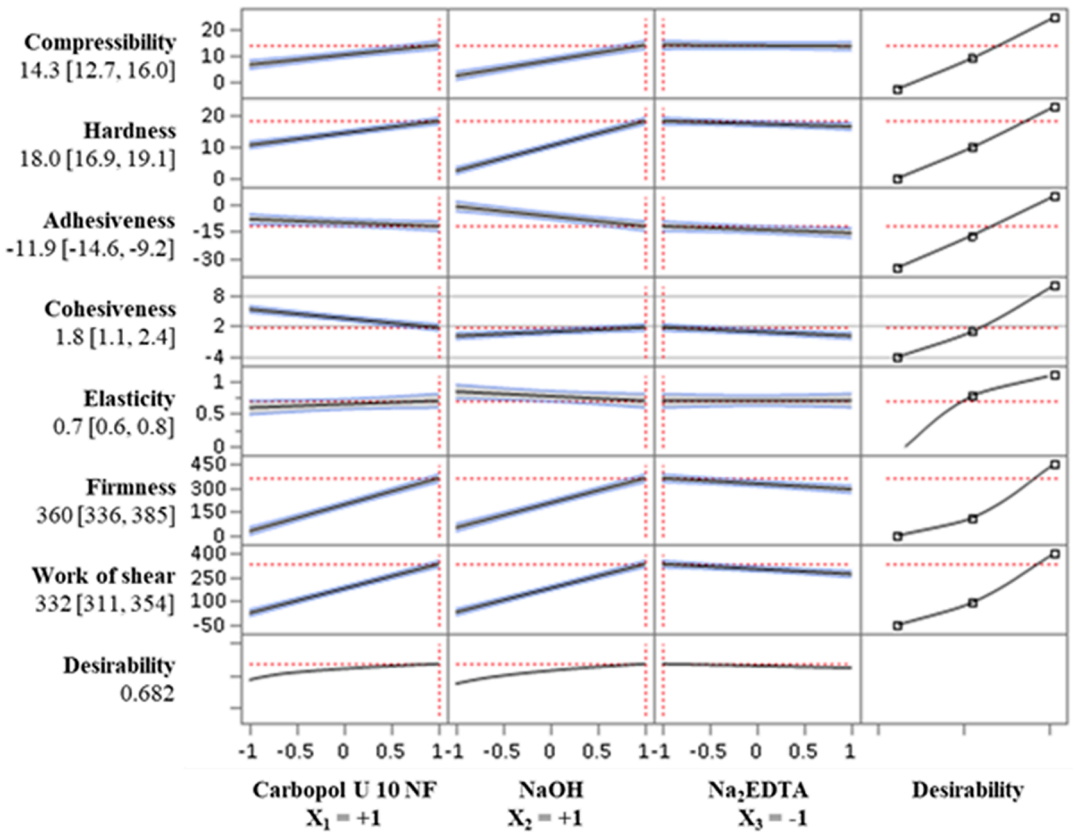

Fig. 2. Overall desirability for hydrogel base composition optimization, according to the target (increase) imposed per mechanical CQA. Average values obtained from Fenistil gel 1 mg/g were considered as reference. The last row of plots shows the desirability trace for each CMA. The overall desirability for all responses is defined as the geometric mean of the desirability functions of the individual responses.

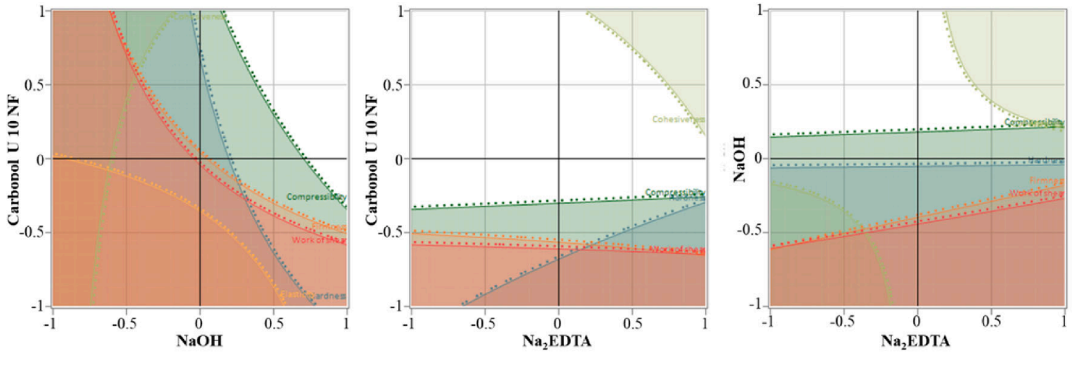

Fig. 3. Optimal working conditions considering the impact of a) X1,X2 (Carbomer, NaOH); b) X1,X3 (Carbomer, Na_2EDTA) and c) X2,X3 (NaOH, Na_2EDTA). Average values obtained from Fenistil Gel 1 mg/g were considered as reference.

type of formulation. Three sets of formulations can be observed: one exhibiting higher viscosity values corresponding to the F6.6. and F6.7; a second one addressing formulations with lower viscosities, including reference and F6.8, and a third one exhibiting formulations with intermediate values of consistency. Also, all the formulations exhibited higher zero-shear viscosity values than the reference. Such a pattern imparts the boundary between gel-like and elastic behavior, reflected in lower or higher values for the yield point ($\tau_{0.ROT}$), as shear stress required to promote the flow of formulations.

Looking at the viscosity at high shear rates (η_{200}) that resembles infinite-shear viscosity behavior, formulations with higher zero-viscosity remain with higher consistency, while those at the intermediate level tend to become closer to the ones presenting inferior viscosity values. This parameter provides information about the formulation behavior after rubbed over the skin surface (Dabbaghi et al., 2021).

All formulations denoted a thixotropic behavior (Fig. 4B and Table 5), as evidenced by the hysteresis loop shape, with F6.1 exhibiting a larger thixotropic relative area. Larger S_R values are indicative of a more structured and consistent hydrogel. Consequently, these are less flowable systems. This means higher shear rates are required to break the system, i.e., more resistance is offered to deformation forces, and more time is demanded to recover its structure, being correlated with formulation spreadability and considered a good stability indicator.

Amplitude sweep tests (Fig. 4C and Table 6) indicated a linear viscoelastic region for all the formulations studied. Rheology profiles of elastic (storage, G') and viscous (loss, G) moduli as a function of shear stress revealed higher G' in comparison with G, supporting their solid behavior, again with F6.6 and F6.7 presenting higher values. The flow

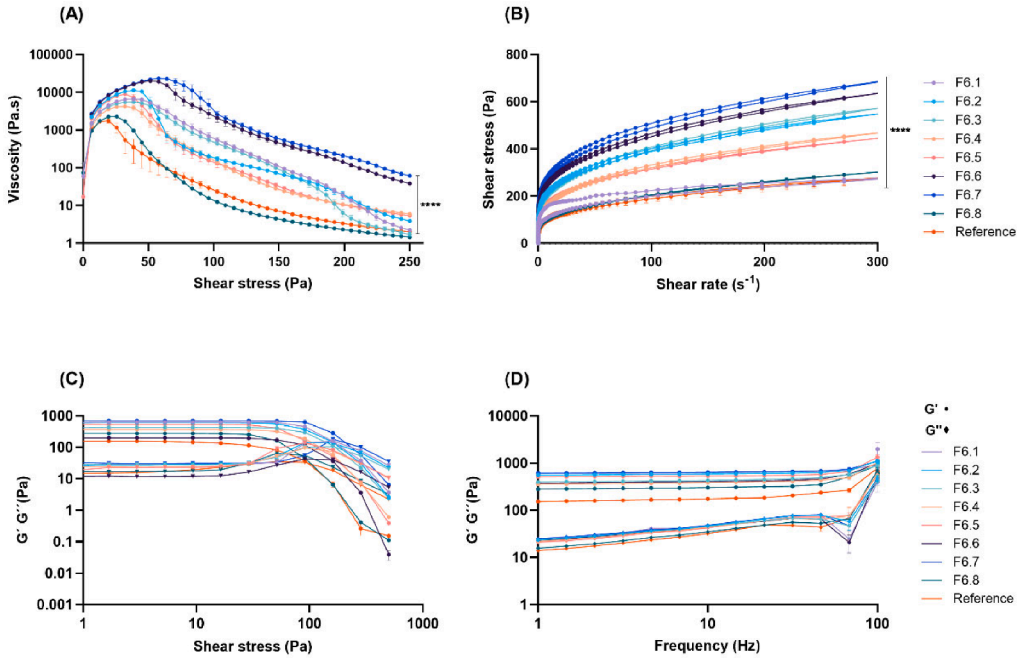

Fig. 4. Rheology profiles of DoE 2 formulations. All results report to mean ± SEM. At least three replicates were used per batch formulation. A) Viscosity curves; B) Thixotropic behavior; C) Amplitude sweep test; D) Frequency sweep test. Statistical significance: ****p < 0,0001, ANOVA analysis, with a Tukey multiple comparison post-test.

Table 5
Parameters extracted from rotational rheological measurements: viscosities at specified shear stresses, comprising zero-shear, shear thinning and infinite-shear viscosity regions (η_i); rotational yield point ($\tau_{0.ROT}$), and thixotropic relative area (S_R), mean ± SD, n = 6.

Formulation	X1′	X2′	X3′	η_{25} (Pa.s)	η_{50} (Pa.s)	η_{100} (Pa.s)	η_{200} (Pa.s)	$\tau_{0.ROT}$ (Pa)	S_R (Pa/s)
F6.1	+	+	+	4836 ± 414	2674 ± 973	152 ± 30	2.6 ± 0.6	69 ± 15	6872 ± 894
F6.2	−	−	−	8741 ± 272	5506 ± 4187	173 ± 50	20 ± 8	46 ± 8	2782 ± 418
F6.3	+	+	−	4964 ± 644	4309 ± 1304	439 ± 135	6 ± 3	71 ± 3	3356 ± 362
F6.4	+	−	−	4163 ± 501	1603 ± 983	140 ± 50	11 ± 1	63 ± 7	2455 ± 226
F6.5	−	−	+	7913 ± 212	2471 ± 2552	129 ± 63	10 ± 2	46 ± 8	1245 ± 216
F6.6	−	+	+	10863 ± 577	19974 ± 700	2098 ± 1148	145 ± 27	74 ± 5	2974 ± 523
F6.7	−	+	−	11335 ± 294	21776 ± 768	2601 ± 954	211 ± 53	77 ± 5	4435 ± 968
F6.8	+	−	+	2255 ± 218	243 ± 53	12 ± 1	2.3 ± 0.2	50 ± 7	671 ± 412
Reference				1715 ± 897	146 ± 92	22 ± 4	2.9 ± 0.4	16.8 ± 0.5	953 ± 132

Key: X1′, Isopropanol; X2′, Carbomer; X3′, NAC/LYS.

Table 6
Parameters extracted from oscillatory amplitude (linear viscoelastic region (**LVR *plateau***); oscillatory yield ($\tau_{0.OSC}$) point and flow point (**τf**)) and frequency (storage modulus (G'), loss modulus (G) and loss tangent (**Tan δ**) at different frequencies) rheological measurements: mean ± SD, n = 6. * SD was considered negligible.

Formulation	Amplitude			Frequency 100 Hz			Frequency 10 Hz			Frequency 1 Hz		
	LVR plateau (ǴPa, 1 Hz)	**τ0.OSC (Pa)**	**τf (Pa)**	**G' (Pa)**	**G (Pa)**	**Tan δ**	**G' (Pa)**	**G (Pa)**	**Tan δ**	**G' (Pa)**	**G (Pa)**	**Tan δ**
F6.1	248 ± 13	51 ± 3	63 ± 42	897 ± 91	542 ± 51	0.6 ± 0.1	405 ± 11	44 ± 6	0.1*	376 ± 20	23 ± 4	0.1*
F6.2	607 ± 31	63 ± 6	137 ± 5	1069 ± 74	435 ± 34	0.41 ± 0.04	592 ± 14	47 ± 3	0.08 ± 0.01	560 ± 12	23 ± 2	0.04*
F6.3	502 ± 38	75 ± 2	104 ± 3	921 ± 90	532 ± 34	0.58 ± 0.08	430 ± 17	46 ± 5	0.11 ± 0.01	399 ± 15	24 ± 3	0.06 ± 0.01
F6.4	364 ± 20	56 ± 7	87 ± 3	933 ± 82	534 ± 35	0.58 ± 0.08	387 ± 16	44 ± 4	0.11 ± 0.01	358 ± 14	22 ± 3	0.06 ± 0.01
F6.5	523 ± 39	46 ± 6	128 ± 5	1139 ± 298	454 ± 140	0.43 ± 0.14	534 ± 20	42 ± 3	0.08 ± 0.01	511 ± 18	21 ± 2	0.04 ± 0.01
F6.6	632 ± 51	75 ± 5	163 ± 7	1011 ± 130	623 ± 97	0.6 ± 0.1	312 ± 22	23 ± 2	0.07 ± 0.01	297 ± 20	12 ± 1	0.04*
F6.7	689 ± 39	108 ± 6	165 ± 8	1075 ± 76	400 ± 78	0.37 ± 0.06	637 ± 25	44 ± 8	0.07 ± 0.01	610 ± 18	25 ± 2	0.04*
F6.8	276 ± 15	35 ± 4	63 ± 2	603 ± 149	541 ± 176	0.9 ± 0.4	303 ± 12	36 ± 4	0.12 ± 0.02	283 ± 10	16 ± 1	0.06 ± 0.01
Reference	374 ± 24	17 ± 3	99 ± 4	1053 ± 167	462 ± 45	0.44 ± 0.04	379 ± 10	72 ± 8	0.19 ± 0.03	335 ± 10	34 ± 6	0.10 ± 0.02

point and the oscillatory yield point retrieved from this test followed the same trend as that previously observed for rotational tests, with F6.1, F6.8 and the reference evidencing lower values to attain a fluid (liquid-like) state (Simões et al., 2020).

The stress sweep tests were performed to find the resistance to deformation at a constant frequency of 1, 10 and 100 Hz (Fig. 4D and Table 6). The loss tangent (tan δ), a dimensionless term that describes the ratio of the loss modulus (G'') to the storage modulus (G') is here an endpoint useful to convey information concerning the structure of the system. When the tan δ approaches zero, the elastic structure of the

system predominates, whereas when it exceeds unity, the system is considered to be primarily viscous (Vitorino et al., 2013) Tan δ values are consistent with amplitude sweep observations, pointing out F6.1 and F6.8 as those showing a more fluid character.

Moreover, most of the oscillatory parameters of the DoE 2 formulations were higher than those of the reference, which consubstantiates a firmer consistency of the tested formulations.

Analysing now the influence of CMAs (Figs. 5 and 6) on the rheological endpoints, it is observed that isopropanol (X1′) is the more impacting factor over the rheological behaviour, followed by the carbomer (X2′) and, lastly, the presence of NAC and LYS (X3′). The addition of isopropanol and the inclusion of the active molecule antagonistically influence viscosity, portraited by the negative coefficient values, whereas the raising in the concentration of the carbomer, reverses this effect. The interaction terms, in particular β_{12}, also reflect a synergistic effect between the isopropanol and the carbomer. Such behaviour is ascribed to the formation of stronger interactions between the carbomer particles in the presence of a water-based gel structure, in comparison to those established for hydroalcoholic gels. Isopropanol is a much less polar solvent in comparison to water, thus requiring higher levels of base to neutralize the system, and consequently enable a swollen state (Kolman et al., 2021).

Fig. 7 depicts a series of two-dimensional plots depicting the presence or absence of interactions among the three DoE 2 CMAs on the significant rheological parameter assessed. The relative slopes of the lines indicate that isopropanol and the carbomer variables crosswise are interacting, which are in agreement with the magnitude of the polynomial coefficients reported in Figs. 5 and 6. The evaluation of the mathematical models that describe the responses is presented in **Figure S2** and **Table S2**, **Supplementary Material**.

Taken together, formulation F6.1 gathers the most promising rheological characteristics that favor a balance between product compliance, in terms of the force required for topical application of the hydrogel, and product stability. This formulation contains the highest concentrations of isopropanol (X1′), carbomer (X2′) and the active molecules (X3′), and was selected for further performance evaluation studies.

3.3. IVRT/IVPT evaluation

The behaviour of NAC and LYS in the hydrogel was assessed through *in vitro* release and permeation testing. Overall, IVRT methods are responsive to product microstructure and provide deeper insights concerning the pharmaceutical performance characteristics of the drug product, whereas IVPT reflects the potential ability of the APIs to penetrate the stratum corneum and reach deeper skin layers. IVRT profiles are displayed in Fig. 8. To meet formal requirements, the release mechanisms of topical products should be represented by the Higuchi model, in which API release exhibits a linear response over the square root of time (Głowińska and Datta, 2014; Marto et al., 2015).

As expected, a lower drug release (μg/cm^2) is observed for the active molecules in the hydrogel, which is consistent with the increased gel viscosity that retards their diffusion to the receptor medium. Furthermore, both molecules follow the Higuchi release mechanism in the F6.1 hydrogel ($R^2 > 0.99$), thereby describing a Fickian behaviour. This indicates that the polymer relaxation time is much greater than the solvent diffusion time. Accordingly, solute transport is controlled by concentration gradients, diffusion distances and degree of swelling (Fu and Kao, 2010). At the end of the study, there is a dose depletion of roughly 17% for each molecule, with a T_{lag} of approximately 0 h.

Regarding the IVPT study, in which the experimental conditions mimic a single application of the F6.1 hydrogel onto the skin, no significant quantity of the active molecules was found in the receptor compartment (below the limit of quantification of the HPLC method). These results indicate neither NAC nor LYS penetrate the stratum corneum, thereby remaining on the skin surface. This is under the product QTPP, in which the active molecules are expected to exert their activity by directly interacting with the allergens, with consequent allergic dermatitis prevention.

3.4. Safety profile of the active ingredients and hydrogel in human keratinocytes

Cell viability was evaluated in keratinocytes, i.e, cells that are representative of the epidermis, in order to evaluate the skin safety profile of the active ingredients alone or formulated in the F6.1 hydrogel. As depicted in Fig. 9, the results demonstrated a lack of significant toxicity for concentrations below 10 mM for NAC and LYS after 24 h of cell treatment. The hydrogel containing the active ingredients followed the same trend, with no significant toxicity in human keratinocytes for all tested concentrations.

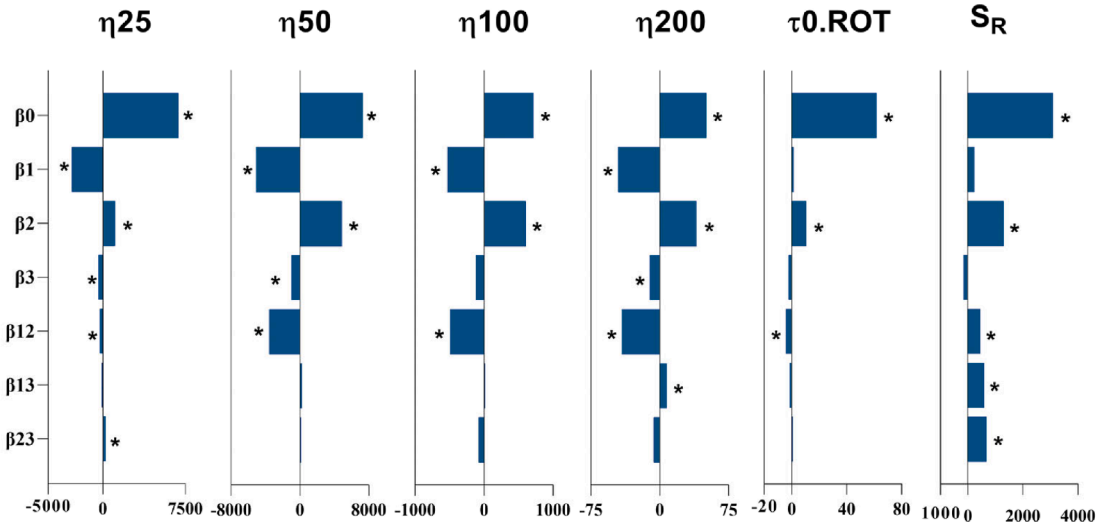

Fig. 5. Coefficients for rotational rheological measurements evaluated in DoE 2 (viscosities at specified shear stresses, comprising zero-shear, shear thinning and infinite-shear viscosity regions (η_i); rotational yield point ($\tau_{0.ROT}$) and thixotropic relative area (S_R)). Key: β_0, intercept; β_1, isopropanol; β_2, Carbomer; β_3, Active molecules; β_{12}, isopropanol*Carbomer; β_{13}, isopropanol*Active molecules; β_{23}, Carbomer*Active molecules. *Statistical significant coefficients, as extracted from Student's *t*-test analysis.

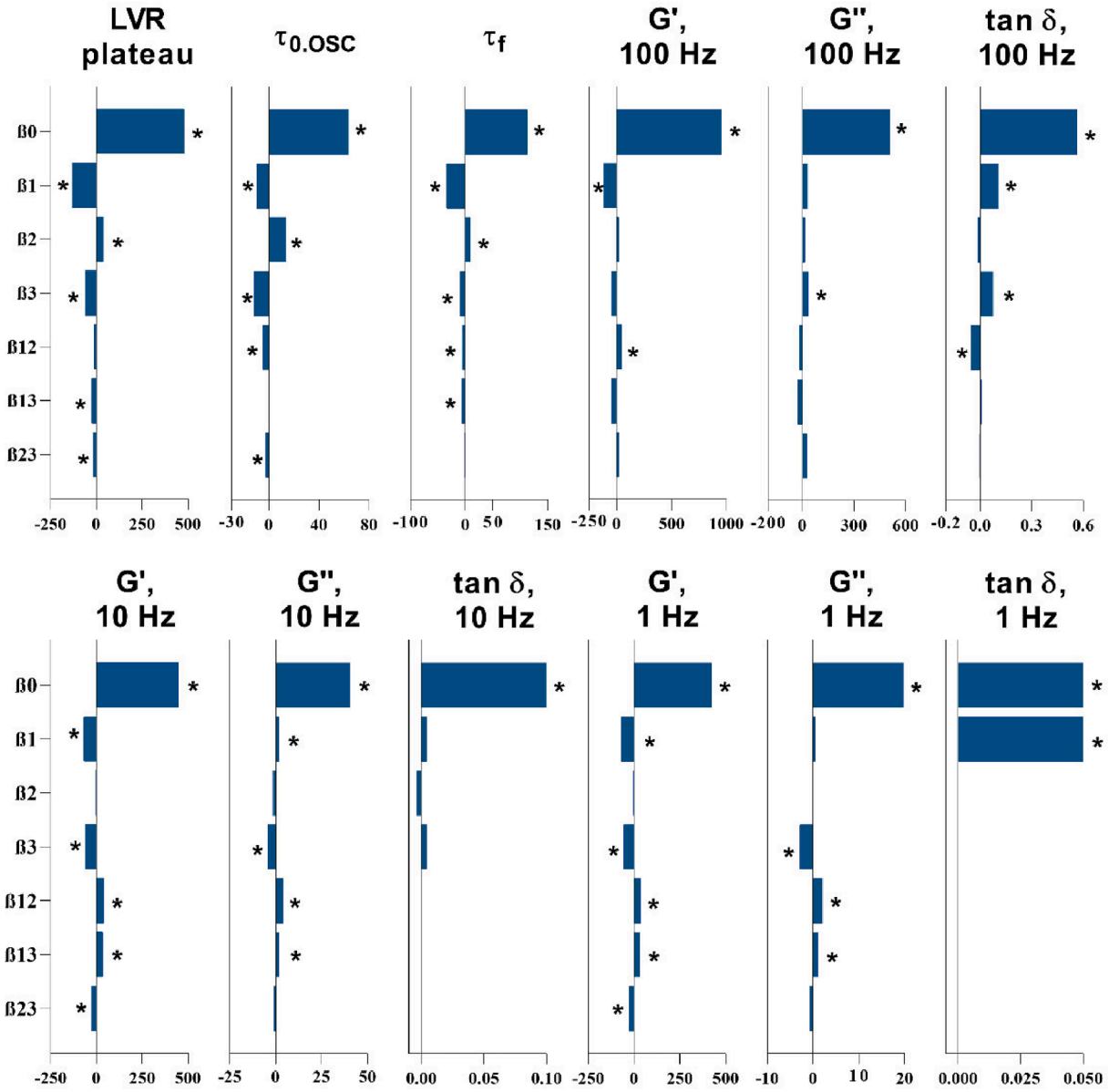

Fig. 6. Coefficients for oscillatory rheological measurements evaluated in DoE 2 (linear viscoelastic region (LVR plateau); oscillatory yield (τ0.OSC) point and storage modulus (τf)) and frequency (storage modulus (G'), loss modulus (G) and loss tangent (Tan δ) at different frequencies). Key: β_0, intercept; β_1, isopropanol; β_2, Carbomer; β_3, Active molecules; β_{12}, isopropanol*Carbomer; β_{13}, isopropanol*Active molecules; β_{23}, Carbomer*Active molecules. *Statistical significant coefficients, as extracted from Student's *t*-test analysis.

3.5. Skin sensitization potential of the active ingredients and effectiveness of the F6.1 hydrogel in THP-1 cells

The requirement of non-animal alternatives has been recognized for the screening of chemicals hazardous to human health, but it has become particularly pressing for cosmetic ingredients due to the full implementation of testing and marketing bans on animal testing under the European Cosmetics Regulation. Fortunately, for some specific endpoints, such as skin sensitization, validated alternatives are already available to be performed during new product development and were herein used to access the safety of the hydrogel containing the active ingredients for human application. Indeed, the THP-1 cell line has been used as a dendritic cell (DC) surrogate for the skin sensitizing hazard, under the OECD guidelines. As such, adapting the OECD Test Guideline No. 442E (OECD, 2022), we evaluated: i) the skin sensitization potential of the hydrogel containing the active ingredients, by assessing changes in CD54 and CD86 protein levels by flow cytometry, ii) the effectiveness of the hydrogel containing the active ingredients after THP-1 cells treatment with the strong skin sensitizers (8 μM) DNFB and (100 μM) MI for 24 h (Fig. 10). Indeed, one of the key events associated with skin sensitization is the maturation of dendritic cells assessed by quantifying the cell surface expression of CD86 and CD54 proteins. As expected, treatment with DNFB and MI, which are strong skin sensitizers, increased the levels of CD54 and CD86. In contrast, the hydrogel formulation did not modify the levels of the co-stimulatory molecules CD54 and CD86, presenting an RFI of CD54 and CD86 lower than 200% and 150%, respectively, therefore ruling out the possibility of evoking skin sensitization. Interestingly, the F6.1 hydrogel was able to mitigate the increase on the co-stimulatory molecule CD54 triggered by DNFB and MI, thus highlighting its potential to rescue skin sensitization.

3.6. Irritation on human skin

We further used the SkinEthic™ Reconstructed Human Epidermis

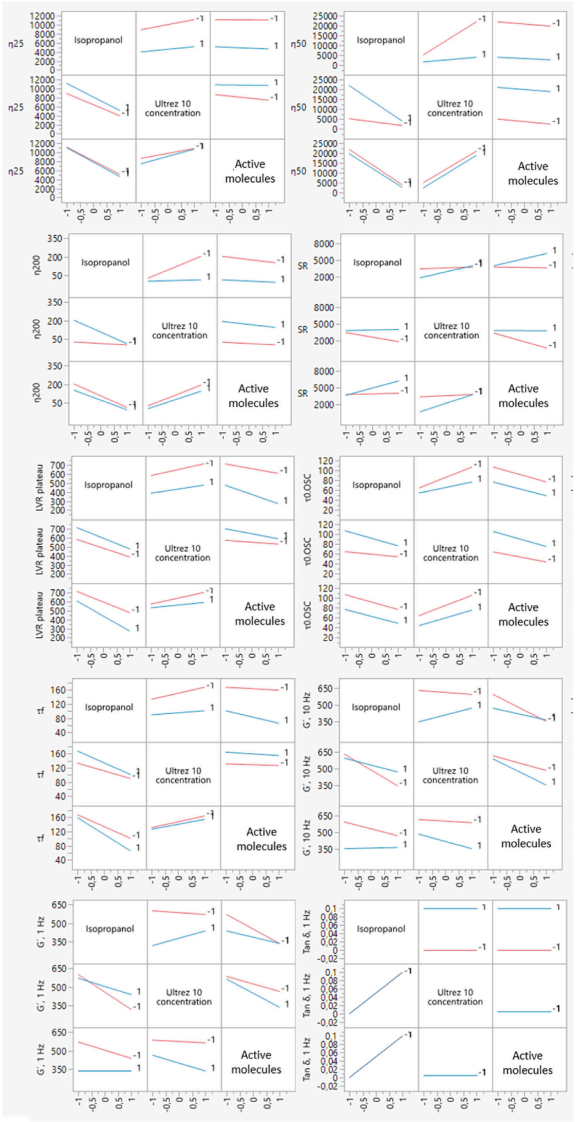

Fig. 7. Interaction plots of the most significant responses in hydrogel rheological assessment. A line segment is plotted for each level of the row effect, and response values predicted by the model are gathered by line segments. Note that non-parallel line segments give visual evidence of possible interactions. However, the *p*-value for such a suggested interaction should be verified to consubstantiate that it exists, see Figs. 5 and 6.

model in compliance with the OECD Test Guideline No. 439, aiming to access if the optimized hydrogel, with or without active ingredients, evokes skin irritation (Fig. 11).

The results (Fig. 11) demonstrated that, as expected, SDS significantly decreased tissue viability (1.49% ± 0.11) when compared to the control (PBS). In contrast, the F6.1 hydrogel, with the active ingredients at 20 mM (98% ± 8) and 100 mM (94% ± 9) did not show any significant irritant activity. Of note, according to ISO 10993-10:2010, the threshold for classifying a substance as non-irritant comprises a tissue viability higher than 50%. These results highlight the safety profile and skin biocompatibility of the formulation enriched with NAC and LYS thus supporting its use in humans for the management of allergic contact dermatitis.

Some hydrogels have already been reported and studied for the treatment of allergic contact dermatitis. Indeed, Kazim and colleagues formulated a chitosan hydrogel for topical delivery of ebastine, an antihistaminic drug that is broadly used to alleviate the symptoms of allergic contact dermatitis. The authors tested the effect of the hydrogel in a BALB/c animal mouse model sensitized with picryl chloride and the results achieved confirmed the success of the hydrogel in alleviating the symptoms of ACD (Kazim et al., 2021). Other formulations have been described to mitigate dermatitis. For instance, barrier creams are important to protect the skin in occupations with chemical exposure. They are designed to provide an obstruction to penetration into the skin of a noxious substance, concomitantly allowing the epidermal barrier to heal while continuing the causative activity (Draelos, 2000). However, they may be too occlusive, decreasing skin barrier function and potentiating allergic contact dermatitis, as reported by Zhai *et al.* An optimal design, like hydrogel, can reduce skin-related dermatitis (Zhai and Maibach, 2001). Indeed, some hydrogels, particularly those enclosing 2-hydroxyethyl methacrylate (Hydron, Hydron Technologies, Boca Raton, FL), can be deposited on the skin as a water-resistant, non-gummy, hygroscopic, flexible, and pliable thin film. These characteristics provide additional efficacy over barrier creams. In a randomized double-blind study of the effects of a cream *versus* a hydrogel vehicle in 80 men, women and children with contact dermatitis, the results demonstrated that the hydrogel resulted in significant improvement in the symptoms of contact dermatitis, compared to the cream-based product. Such effect was ascribed to the well-known ability of hydrogels to form thin, water-resistant, flexible, and stable films on a variety of surfaces. This study also showed that skin can benefit from the qualities above and beyond of simple moisturization of a hydrogel film. Furthermore, the study also demonstrated that some of the hydrogel polymer technology that is currently used in extended-wear soft contact lenses, burns, and ulcers might be valuable in the formulation of barrier/repair creams (Draelos, 2000). Regarding the differences and advantages between a hydrogel and a cream, Trookman and colleagues reported that desonide hydrogel 0.05% is as effective at reducing the symptoms of mild-to-moderate

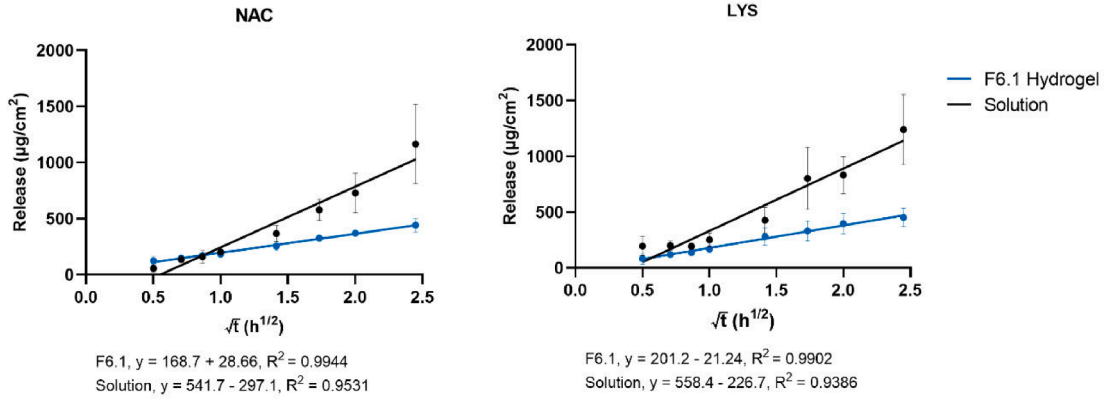

Fig. 8. In vitro release testing profiles for NAC and LYS in the optimized hydrogel (F6.1) and solution. Results are expressed as mean ± SD (n = 6).

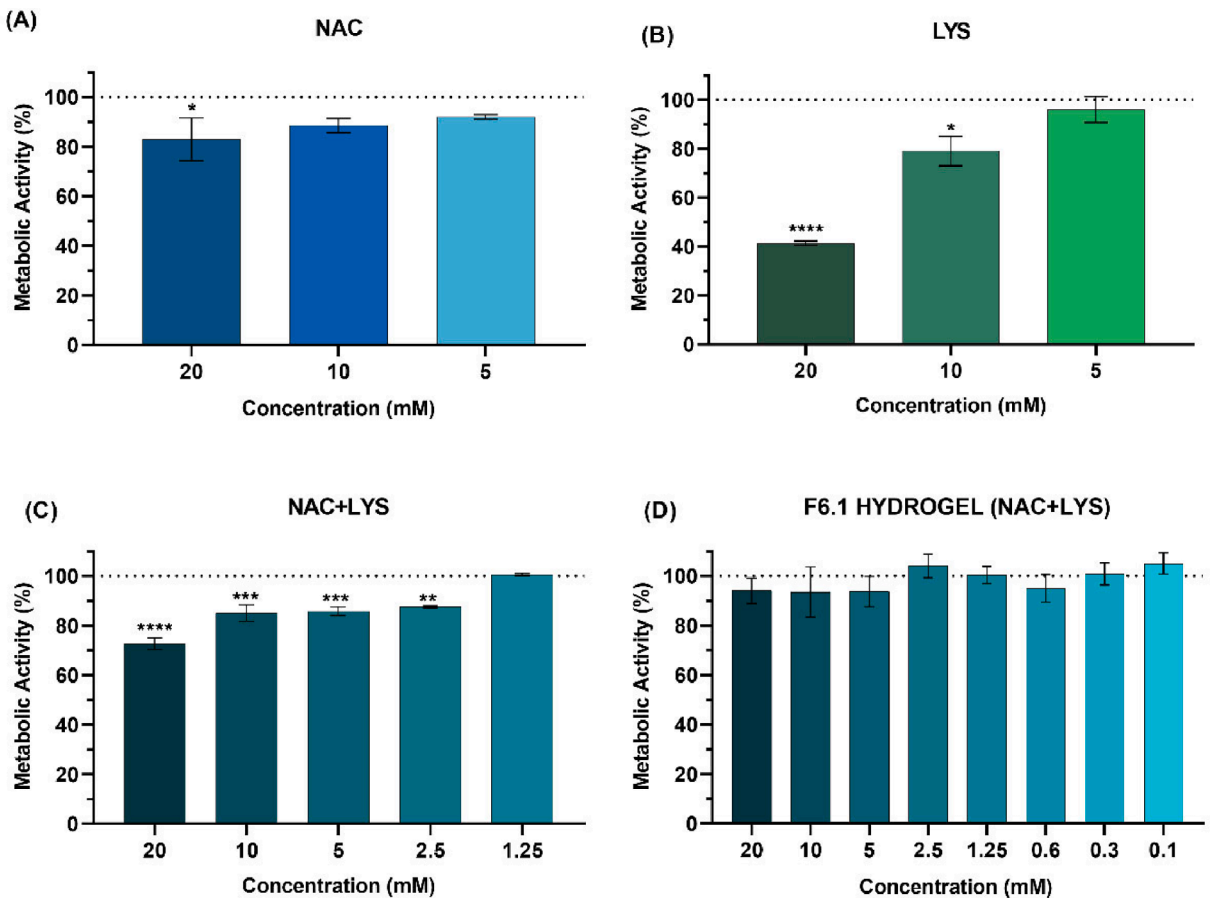

Fig. 9. Effect of NAC, LYS, NAC + LYS and the F6.1 hydrogel with NAC + LYS on HaCaT cell viability. Cells were treated for 24 h with different concentrations of NAC (A), LYS (B), NAC + LYS (C) or the hydrogel containing increasing concentrations of the active ingredients (D), with viability being evaluated by the resazurin reduction assay. The results were expressed as percentage (%) of cell viability relatively to control and represent the mean ± SEM of at least 3 independent experiments performed in triplicate. Statistical analysis was made by one-way analysis of variance (ANOVA) followed by Dunnett's multiple comparison test.

contact dermatis as a desonide ointment 0.05% preparation, but it promotes superior patient compliance when compared to the ointment, due to better absorbability and lack of greasiness(Trookman et al., 2011). All these studies support the development of hydrogel formulations containing new active ingredients for the management of allergic contact dermatitis.

4. Conclusion

In this study, we have developed a new hydrogel formulation with the potential to prevent allergic contact dermatitis by hindering the penetration and reactivity of allergens with skin proteins, therefore functioning like a "chemical glove". To this end, L-lysine and N-acetyl cysteine, previously highlighted by the team as active ingredients with high antiallergic potential, were incorporated within a hydrogel-based device. This formulation has spreadability and sensory characteristics suitable for human skin and patient compliance. The battery of studies regarding product performance showed that the active molecules can be released from the hydrogel and remain on the surface of the epidermis. In addition, the *in vitro* studies highlight the safety profile and skin biocompatibility of the optimized formulation, thus supporting its use in humans for the management of allergic contact dermatitis. Furthermore, the developed hydrogel could be used alone or in combination with other preventive approaches, as well as be incorporated into cosmetic and pharmaceutical products opening new avenues for the prevention and management of allergic contact dermatitis.

Patents

Part of this work was involved in one provisional patent application (20221000002771).

Funding

This work was financially supported by the European Regional Development Fund (ERDF), through the Centro 2020 Regional Operational Programme under project CENTRO-01-0145-FEDER-000012 (HealthyAging2020) and through the COMPETE 2020 - Operational Programme for Competitiveness and Internationalization and Portuguese national funds via FCT – Fundação para a Ciência e a Tecnologia, under project POCI-01-0145-FEDER-029369, UID/NEU/04539/2019 and UID/QUI/00313/2020. Thanks are due to FCT/FEDER/COMPETE2020 for the financial support of iBiMED (UIDB/04501/2020). Gonçalo Brites, João Basso and Margarida Miranda are supported by FCT through an individual PhD fellowship (PD/BDE/142926/2018, SFRH/BD/149138/2019 and PD/BDE/135075/2017, respectively).

CRediT authorship contribution statement

Gonçalo Brites: Conceptualization, Methodology, Formal analysis, Investigation, Writing – original draft. **João Basso:** Conceptualization, Methodology, Formal analysis, Visualization, Writing – original draft. **Margarida Miranda:** Methodology, Writing – original draft. **Bruno Miguel Neves:** Supervision, Project administration, Funding acquisition, Writing – review & editing. **Carla Vitorino:** Conceptualization, Methodology, Formal analysis, Validation, Supervision, Project administration, Funding acquisition, Writing – original draft, Writing – review & editing. **Maria Teresa Cruz:** Supervision, Project administration,

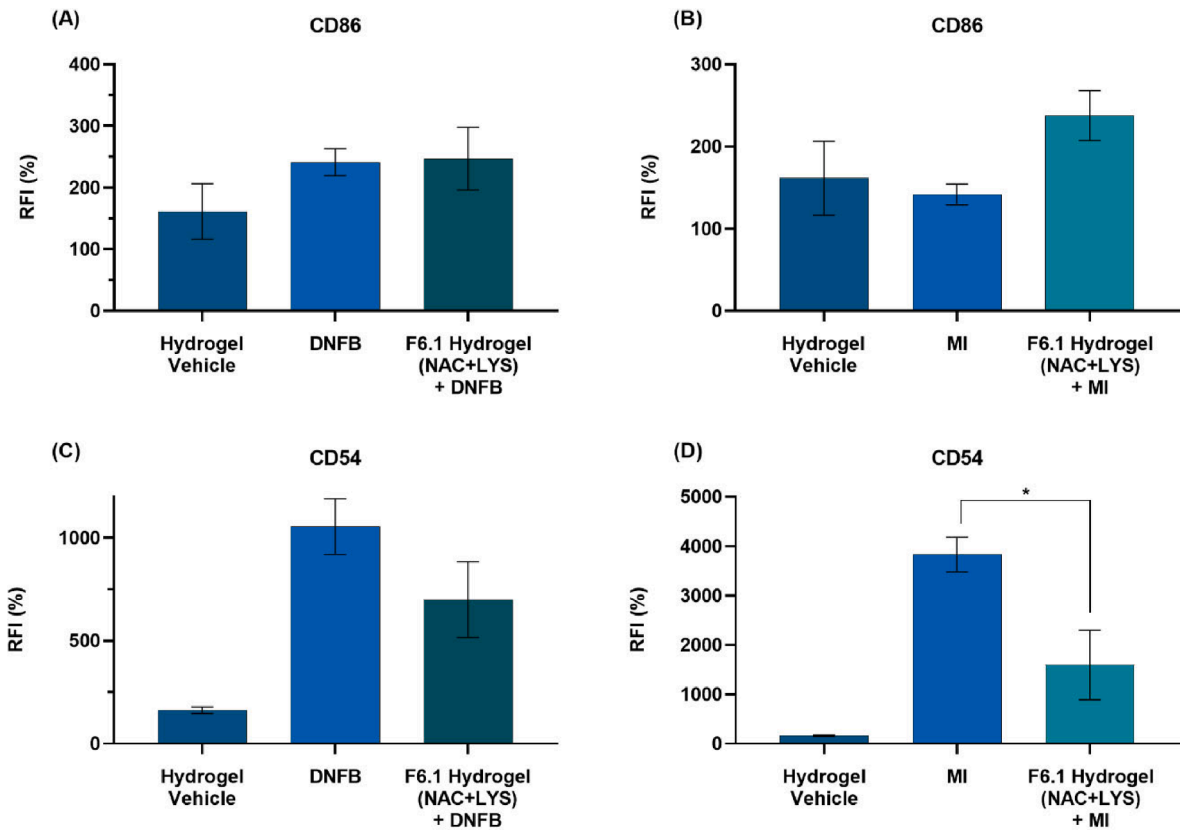

Fig. 10. Effect of the hydrogel containing the active ingredients on the levels of the co-stimulatory proteins CD86 (A,B) and CD54 (C,D) in THP-1 monocytes. Skin sensitization was induced with two strong allergens: DNFB (8 μM) (A, C) and MI (B, D) (100 μM), for 24 h. The expression of CD54 and CD86 was measured by flow cytometry. The results were expressed as percentage (%) of relative fluorescent intensity (RFI) relatively to control and represent the mean ± SEM of at least 3 independent experiments. Statistical analysis was made by one-way analysis of variance (ANOVA) followed by Dunnett's and Sidak's multiple comparison tests. * $p < 0.05$.

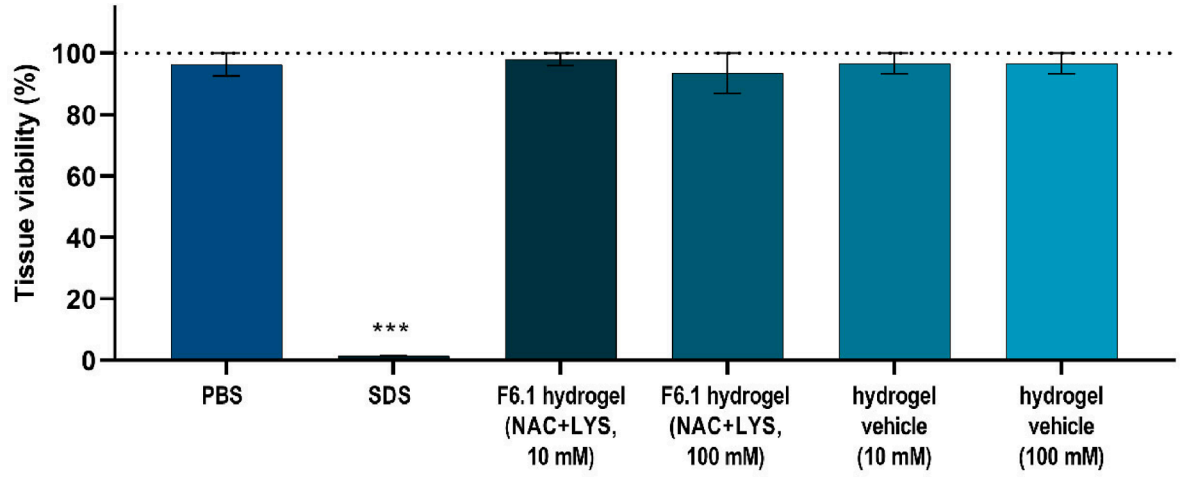

Fig. 11. Effect of the hydrogel formulation on tissue viability in Reconstructed Human Epidermis. The inserts were treated with PBS (negative control), or 5% SDS (positive control), or in the absence or presence of the active ingredients (20 and 100 mM) for 42 min. Tissue viability was assessed by the MTT assay. Results were expressed as a percentage (%) of the tissue viability relative to the control and represent the mean ± SEM of at least three independent experiments. The statistical analysis was performed by one-way ANOVA, followed by Dunnett's multiple comparison test. *** $p < 0.0001$: significant different compared to the control.

Funding acquisition, Writing – original draft.

Declaration of Competing Interest

MTC, CV, BN and GB have patent #Topical Composition and Uses Thereof (20221000002771) pending to University of Coimbra / ToxFinder.Lda.

Data availability

Data will be made available on request.

Appendix A. Supplementary material

Supplementary data to this article can be found online at https://doi.org/10.1016/j.ijpharm.2022.122265.

References

Basso, J., Ramos, M.L., Pais, A., Vitorino, R., Fortuna, A., Vitorino, C., 2021. Expediting Disulfiram Assays through a Systematic Analytical Quality by Design Approach. Chemosensors 2021, Vol. 9, Page 172 9, 172. https://doi.org/10.3390/CHEMOSENSORS9070172.

Brites, G.S., Ferreira, I., Sebastião, A.I., Silva, A., Carrascal, M., Neves, B.M., Cruz, M.T., 2020. Allergic contact dermatitis: From pathophysiology to development of new preventive strategies. Pharmacological Research 162. https://doi.org/10.1016/j.phrs.2020.105282.

Coenraads, P.J., Vogel, T.A., Blömeke, B., Goebel, C., Roggeband, R., Schuttelaar, M.L.A., 2016. The role of the antioxidant ascorbic acid in the elicitation of contact allergic reactions to p -phenylenediamine. Contact Dermatitis 74, 267–272. https://doi.org/10.1111/cod.12535.

Dabbaghi, M., Namjoshi, S., Panchal, B., Grice, J.E., Prakash, S., Roberts, M.S., Mohammed, Y., 2021. Viscoelastic and deformation characteristics of structurally different commercial topical systems. Pharmaceutics 13, 1–11. https://doi.org/10.3390/pharmaceutics13091351.

Draelos, Z.D., 2000. Hydrogel barrier/repair creams and contact dermatitis. Am. J. Contact Dermatitis 11, 222–225. https://doi.org/10.1053/ajcd.2000.8586.

Fluhr, J.W., Darlenski, R., 2014. Transepidermal water loss (TEWL). In: Berardesca, E., Maibach, H.I., Wilhelm, K.-P. (Eds.), Non Invasive Diagnostic Techniques in Clinical Dermatology. Springer Berlin Heidelberg, Berlin, Heidelberg, pp. 353–356.

Fu, Y., Kao, W.J., 2010. Drug release kinetics and transport mechanisms of non-degradable and degradable polymeric delivery systems. Expert Opin. Drug Deliv. 7, 429–444. https://doi.org/10.1517/17425241003602259.

Głowińska, E., Datta, J., 2014. A mathematical model of rheological behavior of novel bio-based isocyanate-terminated polyurethane prepolymers. Ind. Crops Prod. 60, 123–129. https://doi.org/10.1016/J.INDCROP.2014.06.016.

Harrison, I., Spada, F., 2018. Hydrogels for atopic dermatitis and wound management: A superior drug delivery vehicle. Pharmaceutics 10 (2), 71.

Horinouchi, C.D.D.S., Mendes, D.A.G.B., Soley, B.D.S., Pietrovski, E.F., Facundo, V.A., Santos, A.R.S., Cabrini, D.A., Otuki, M.F., 2013. Combretum leprosum Mart. (Combretaceae): potential as an antiproliferative and anti-inflammatory agent. J. Ethnopharmacol. 145, 311–319. https://doi.org/10.1016/J.JEP.2012.10.064.

Hurler, J., Engesland, A., Poorahmary Kermany, B., Škalko-Basnet, N., 2012. Improved texture analysis for hydrogel characterization: Gel cohesiveness, adhesiveness, and hardness. J. Appl. Polym. Sci. 125, 180–188. https://doi.org/10.1002/app.35414.

Jenkinson, C., Jenkins, R.E., Maggs, J.L., Kitteringham, N.R., Aleksic, M., Park, B.K., Naisbitt, D.J., 2009. A mechanistic investigation into the irreversible protein binding and antigenicity of p-phenylenediamine. Chem. Res. Toxicol. 22, 1172–1180. https://doi.org/10.1021/tx900095r.

Kalariya, P.D., Namdev, D., Srinivas, R., Gananadhamu, S., 2017. Application of experimental design and response surface technique for selecting the optimum RP-HPLC conditions for the determination of moxifloxacin HCl and ketorolac tromethamine in eye drops. J. Saudi Chem. Soc. 21, S373–S382. https://doi.org/10.1016/j.jscs.2014.04.004.

Kamal, N., Krishnaiah, Y., Xu, X., Zidan, A., Sameersingh, R., Cruz, C., Ashraf, M., 2020. Identification of critical formulation parameters affecting the in vitro release, permeation, and rheological properties of the acyclovir topical cream. International Journal of Pharmaceutics 590 (30 November 2020). https://doi.org/10.1016/j.ijpharm.2020.119914.

Kamboj, S., Rana, V., 2016. Quality-by-design based development of a self-microemulsifying drug delivery system to reduce the effect of food on Nelfinavir mesylate. Int. J. Pharm. 501, 311–325. https://doi.org/10.1016/j.ijpharm.2016.02.008.

Kazim, T., Tariq, A., Usman, M., Ayoob, M.F., Khan, A., 2021. Chitosan hydrogel for topical delivery of ebastine loaded solid lipid nanoparticles for alleviation of allergic contact dermatitis. RSC Adv. 11, 37413–37425. https://doi.org/10.1039/d1ra06283b.

Kolman, M., Smith, C., Chakrabarty, D., Amin, S., 2021. Rheological stability of carbomer in hydroalcoholic gels: Influence of alcohol type. Int. J. Cosmet. Sci. 43, 748–763. https://doi.org/10.1111/ICS.12750.

Kryscio, D.R., Sathe, P.M., Lionberger, R., Yu, L., Bell, M.A., Jay, M., Hilt, J.Z., 2008. Spreadability Measurements to Assess Structural Equivalence (Q3) of Topical Formulations—A Technical Note. AAPS PharmSciTech 9, 84–86. https://doi.org/10.1208/s12249-007-9009-5.

Kulkarni, V.S., Shaw, C., 2016. Use of Polymers and Thickeners in Semisolid and Liquid Formulations. In: Essential Chemistry for Formulators of Semisolid and Liquid Dosages. Academic Press, pp. 43–69. https://doi.org/10.1016/b978-0-12-801024-2.00005-4.

Lubrizol, 2011. Bulletin 3- Polymer Handling and Storage [WWW Document]. URL www.pharma.lubrizol.com (accessed 4.5.22).

Machado, V.S., Camponogara, C., Oliveira, S.M., Baldissera, M.D., Sagrillo, M.R., Gundel, S.DA.S., Silva, A.P.T.DA., Ourique, A.F., Klein, B., Wagner, R., Santos, R.C.V., Silva, A.S.DA., 2020. Topical hydrogel containing achyrocline satureioides oily extract (Free and nanocapsule) has anti-inflammatory effects and thereby minimizes irritant contact dermatitis. Anais da Academia Brasileira de Ciencias 92 (4). https://doi.org/10.1590/0001-3765202020191066.

Marto, J., Baltazar, D., Duarte, A., Fernandes, A., Gouveia, L., Militão, M., Salgado, A., Simões, S., Oliveira, E., Ribeiro, H.M., 2015. Topical gels of etofenamate: in vitro and in vivo evaluation. Pharm. Dev. Technol. 20, 710–715. https://doi.org/10.3109/10837450.2014.915571.

Miranda, M., Cova, T., Augusto, C., Pais, A.A.C.C., Cardoso, C., Vitorino, C., 2020. Diving into Batch-to-Batch Variability of Topical Products-a Regulatory Bottleneck. Pharm. Res. 37 https://doi.org/10.1007/s11095-020-02911-y.

Miranda, M., Pais, A.A.C.C., Cardoso, C., Vitorino, C., 2019. aQbD as a platform for IVRT method development – A regulatory oriented approach. Int. J. Pharm. 572, 118695 https://doi.org/10.1016/j.ijpharm.2019.118695.

Narayanaswamy, R., Torchilin, V.P., 2019. Hydrogels and their applications in targeted drug delivery. Molecules 24 (3), 603.

O'Brien, J., Wilson, I., Orton, T., Pognan, F., 2000. Investigation of the Alamar Blue (resazurin) fluorescent dye for the assessment of mammalian cell cytotoxicity. Eur. J. Biochem. 267, 5421–5426. https://doi.org/10.1046/j.1432-1327.2000.01606.x.

OECD, 2022. Test No. 442E: In Vitro Skin Sensitisation, OECD Guidelines for the Testing of Chemicals, Section 4. OECD. https://doi.org/10.1787/9789264264359-en.

Parrado, C., Mercado-Saenz, S., Perez-Davo, A., Gilaberte, Y., Gonzalez, S., Juarranz, A., 2019. Environmental Stressors on Skin Aging, Mechanistic Insights. Front. Pharmacol. 10, 759. https://doi.org/10.3389/FPHAR.2019.00759/BIBTEX.

Shin, S.H., Rantou, E., Raney, S.G., Ghosh, P., Hassan, H., Stinchcomb, A., 2020. Cutaneous Pharmacokinetics of Acyclovir Cream 5% Products: Evaluating Bioequivalence with an In Vitro Permeation Test and an Adaptation of Scaled Average Bioequivalence. Pharm. Res. 37 https://doi.org/10.1007/s11095-020-02821-z.

Simões, A., Miranda, M., Cardoso, C., Veiga, F., Vitorino, C., 2020. Rheology by design: A regulatory tutorial for analytical method validation. Pharmaceutics 12, 1–27. https://doi.org/10.3390/pharmaceutics12090820.

Simões, A., Veiga, F., Vitorino, C., 2019. Developing Cream Formulations: Renewed Interest in an Old Problem. J. Pharm. Sci. 108, 3240–3251. https://doi.org/10.1016/J.XPHS.2019.06.006.

Trookman, N.S., Rizer, R.L., Ho, E.T., Ford, R.O., Gotz, V., 2011. Moisturizing advantages of desonide hydrogel in treating atopic dermatitis. Cutis; cutaneous medicine for the practitioner 88, 7–12.

Unzueta, A., Vargas, H.E., 2013. Nonsteroidal anti-inflammatory drug-induced hepatoxicity. Clin. Liver Dis. 17, 643–656. https://doi.org/10.1016/J.CLD.2013.07.009.

Uter, W., Werfel, T., White, I.R., Johansen, J.D., 2018. Contact Allergy : A Review of Current Problems from a Clinical Perspective. Int. J. Environ. Res. Public Health. https://doi.org/10.3390/ijerph15061108.

Varges, P.R., Costa, C.M., Fonseca, B.S., Naccache, M.F., De Souza Mendes, P., 2019. Rheological characterization of carbopol ® dispersions in water and in water/glycerol solutions. Fluids 4 (1), 3.

Vitorino, C., Almeida, A., Sousa, J., Lamarche, I., Gobin, P., Marchand, S., Couet, W., Olivier, J.C., Pais, A., 2014. Passive and active strategies for transdermal delivery using co-encapsulating nanostructured lipid carriers: In vitro vs. in vivo studies. Eur. J. Pharm. Biopharm. 86, 133–144. https://doi.org/10.1016/J.EJPB.2013.12.004.

Vitorino, C., Alves, L., Antunes, F.E., Sousa, J.J., Pais, A.A.C.C., 2013. Design of a dual nanostructured lipid carrier formulation based on physicochemical, rheological, and mechanical properties. J. Nanopart. Res. 15 https://doi.org/10.1007/s11051-013-1993-7.

Yeom, M., Kim, S.H., Lee, B., Han, J.J., Chung, G.H., Choi, H.D., Lee, H., Hahm, D.H., 2012. Oral administration of glucosylceramide ameliorates inflammatory dry-skin condition in chronic oxazolone-induced irritant contact dermatitis in the mouse ear. J. Dermatol. Sci. 67, 101–110. https://doi.org/10.1016/J.JDERMSCI.2012.05.009.

Zhai, H., Maibach, H.I., 2001. Skin occlusion and irritant and allergic contact dermatitis: an overview. Contact Dermatitis 44, 201–206. https://doi.org/10.1034/J.1600-0536.2001.044004201.X.